Self-Assembling Properties of Porphyrinic Photosensitizers and Their Effect on Membrane Interactions Probed by NMR Spectroscopy

ARTICLE *in* THE JOURNAL OF PHYSICAL CHEMISTRY B · MAY 2013

Impact Factor: 3.3 · DOI: 10.1021/jp403331n · Source: PubMed

3 AUTHORS, INCLUDING:

Martina Vermathen
Universität Bern
22 PUBLICATIONS **515** CITATIONS
SEE PROFILE

Peter Bigler
Universität Bern
65 PUBLICATIONS **887** CITATIONS
SEE PROFILE

THE JOURNAL OF PHYSICAL CHEMISTRY B

Article

pubs.acs.org/JPCB

Self-Assembling Properties of Porphyrinic Photosensitizers and Their Effect on Membrane Interactions Probed by NMR Spectroscopy

Martina Vermathen,* Mattia Marzorati, and Peter Bigler

Department of Chemistry and Biochemistry, University of Bern, Freiestrasse 3, CH-3012 Bern, Switzerland

Supporting Information

ABSTRACT: Aggregation and membrane penetration of porphyrinic photosensitizers play crucial roles for their efficacy in photodynamic therapy. The current study was aimed at comparing the aggregation behavior of selected photosensitizers and correlating it with membrane affinity. Self-assembling properties of 15 amphiphilic free-base chlorin and porphyrin derivatives bearing carboxylate substituents were studied in phosphate buffered saline (PBS) by ^{1}H NMR spectroscopy, making use of ring current induced aggregation shifts. All compounds exhibited aggregation in PBS to a different degree with dimers or oligomers showing slow aggregate growth over time. Aggregate structures were proposed on the basis of temperature dependent chemical shift changes. All chlorin compounds revealed similar aggregation maps with their hydrophobic sides overlapping and their carboxylate groups protruding toward the exterior. In contrast, for the porphyrin compounds, the carboxylate groups were located in overlapping regions. Membrane interactions were probed using 1,2-dioleoyl-*sn*-glycero-3-phosphocholine (DOPC) bilayer vesicles and 1,2-dihexanoyl-*sn*-glycero-3-phosphocholine (DHPC) micelles as models. The chlorin derivatives had higher membrane affinity and were all monomerized by DHPC micelles as opposed to the porphyrin compounds. The observed differences were attributed to the different aggregate structures proposed for the chlorin and porphyrin derivatives. Free accessibility of the carboxylate groups seemed to promote initial surface interaction with phospholipid bilayers and micelles.

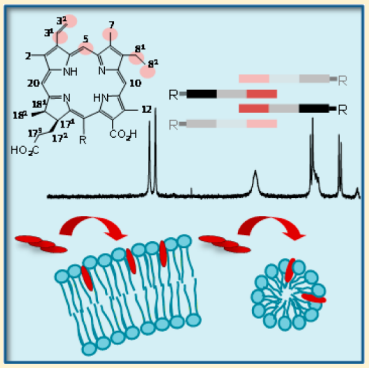

INTRODUCTION

Porphyrinic compounds play an important role as photosensitizers in photodynamic therapy (PDT) of cancer and other noncancerous diseases. PDT is based on the combination of a photosensitizer, light, and oxygen leading to a phototoxic reaction in the target tissue. As a highly selective, minimally invasive treatment modality, PDT has thus become a promising alternative to conventional cancer therapy.[1,2] Porphyrinic compounds comprise several properties which render them preferential candidates as photosensitizers: they accumulate in diseased, proliferative tissue, and they are phototoxic upon light irradiation and singlet oxygen formation, while their dark toxicity is generally low.[3,4] However, owing to their more or less hydrophobic and planar aromatic ring structures, porphyrins have a high tendency for self-association in aqueous solutions. Aggregation under physiological conditions observed for many porphyrinic photosensitizers is a main limitation in PDT.[5−7] It reduces their water solubility, singlet oxygen quantum yields, and thus also their PDT efficacy. Since membranes belong to the main cellular and subcellular targets of porphyrinic photosensitizers,[2,4] a certain lipophilicity is required for optimal membrane penetration. Therefore, hydrophilic and lipophilic properties have to be balanced to reduce aggregation and enhance membrane solubility at the same time.

In current porphyrin research, several strategies are being pursued to prevent porphyrin aggregation. Chemical modification, e.g., linkage of bulky substituents[8−10] or metal coordination,[10,11] and use of drug delivery vehicles,[5,12] like liposomes or polymeric nanoparticles, are different approaches to overcome the unfavorable effects of porphyrin aggregation.

Porphyrin aggregation has been well studied by NMR spectroscopic methods starting with the early work of Abraham and Hunter.[13−16] Typical ring current induced ^{1}H NMR shifts are indicative of aggregate formation and are thus well suited to study the extent and structure of the supra-molecular assemblies formed in solution. While in metal porphyrins the central metal ion plays a major role in aggregate formation, in free base porphyrins, weak $\pi-\pi$-interactions between the aromatic macrocycles are the main contributors[17] besides interactions involving ring substituents.

A lot of aggregate structures for specific porphyrin or chlorin compounds under various conditions have been reported in the literature.[7,18−23] It has been shown that small changes in the porphyrin structure like the length of alkyl substituents can have a significant impact on the aggregation behavior.[20,21,24] Moreover, the nature of the aggregate formed depends on factors such as porphyrin concentration, solvent, ionic strength, pH of the surrounding medium, and temperature.[17] It is therefore hard to predict what type of aggregate is formed for a

Received: April 4, 2013
Revised: May 16, 2013

   dx.doi.org/10.1021/jp403331n | *J. Phys. Chem. B* XXXX, XXX, XXX−XXX

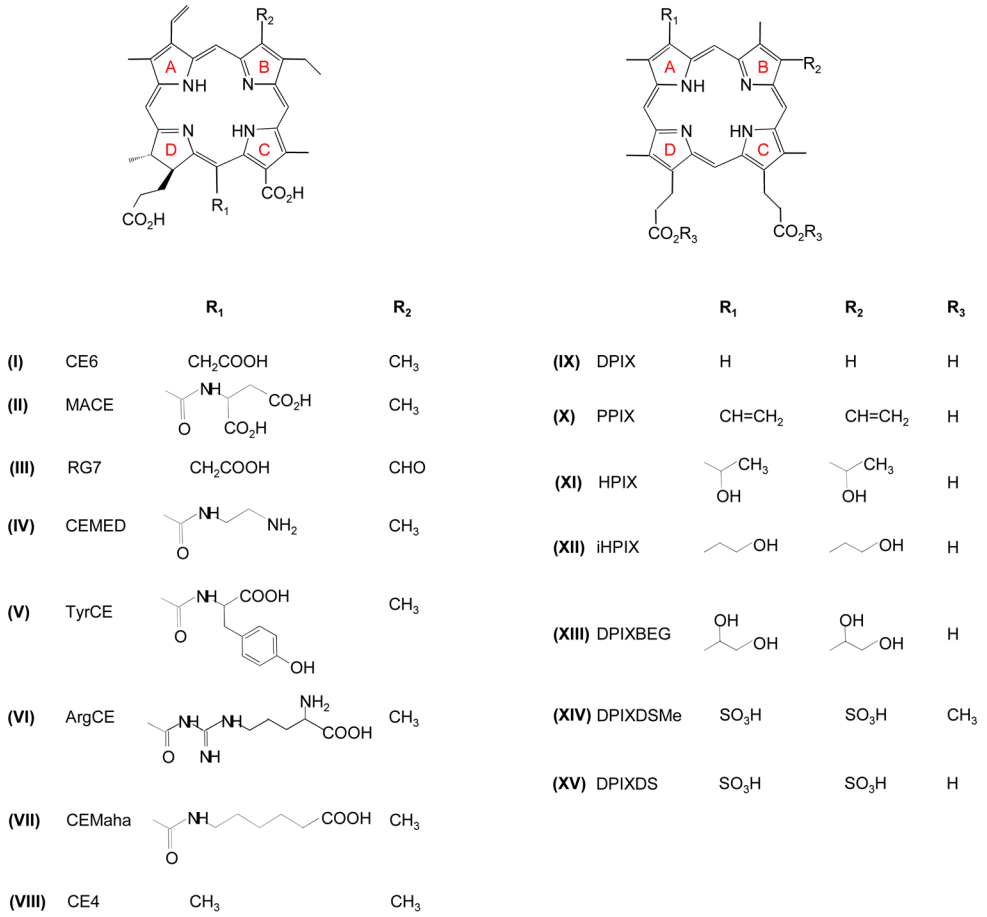

Figure 1. Chemical structures of the chlorin (I–VIII) and porphyrin (IX–XV) derivatives.

given porphyrin and how this aggregation behavior modulates membrane uptake.

Therefore, the aim of the current work was to probe the relationship between porphyrin substitution pattern, aggregate structure, and membrane affinity under well-defined conditions in a systematic comparative study. For this, a total of 15 different but structurally similar free base porphyrin and chlorin compounds were analyzed with respect to their aggregation behavior under the same physiological conditions, i.e., at neutral pH and constant ionic strength (0.9% NaCl). As outlined above, NMR spectroscopy has proved to be a powerful tool for a detailed characterization of porphyrin aggregates. Therefore, in the current paper, qualitative and semiquantitative self-assembling properties were studied and correlated with membrane interactions using ^{1}H NMR spectroscopy. Information on the extent of aggregation as well as on the stability, structure, and size of the aggregates formed was obtained. In view of their importance for PDT, membrane interactions were probed in the presence of long chain phospholipid bilayers and short chain phospholipid micelles. Knowledge of the aggregation behavior and its correlation with membrane interactions may be important for estimating porphyrin PDT efficacy and for the development of appropriate drug formulations.

EXPERIMENTAL SECTION

Materials. The porphyrinic compounds chlorin e6 (CE6, I), mono-L-aspartyl-chlorin e6 tetrasodium salt (MACE, II), rhodin G7 sodium salt (RG, III), chlorin e6 monoethylene diamine monoamide disodium salt (CEMED, IV), monotyrosine amide of chlorin e6 trisodium salt (TyrCE, V), arginine amide of chlorin e6 trisodium salt (ArgCE, VI), chlorin e6 mono 6-amino hexanoic acid amide (CEMaha, VII), chlorin e4 (CE4, VIII), deuteroporphyrin IX dihydrochloride (DPIX, IX), protoporphyrin IX (PPIX, X), hematoporphyrin IX base (HPIX, XI), isohematoporphyrin IX (iHPIX, XII), deuteroporphyrin IX 2,4 bis ethylene glycol (DPIXBEG, XIII), deuteroporphyrin IX 2,4-disulfonic acid dimethyl ester disodium salt (DPIXDSME, XIV), and deuteroporphyrin IX 2,4-disulfonic acid dihydrochloride (DPIXDS, XV) were purchased from Frontier Scientific. The structures of the chlorin and porphyrin compounds are shown in Figure 1. 18:1 PC (cis) 1,2-dioleoyl-*sn*-glycero-3-phosphocholine (DOPC) and 6:0 PC 1,2-dihexanoyl-*sn*-glycero-3-phosphocholine (DHPC) were purchased from Avanti Polar Lipids Inc. The deuterated solvents D_2O (D 99.9%) and DMSO-*d6* were obtained from Cambridge Isotopes Laboratories, Inc. Trimethyl-silyl-3-propionic acid sodium salt D4 (*d*4-TMSP, D 98%), obtained from Euriso-Top, was used as the internal ^{1}H NMR reference. All chemicals and solvents were used without further purification. All porphyrin stock solutions were freshly prepared in D_2O or DMSO-*d6* at a concentration of 15 mM. Phosphate buffered saline (PBS) solution of neutral pH (pH 7) was prepared by mixing aliquots of 10 mM solutions of KH_2PO_4 and Na_2HPO_4 (both Sigma-Aldrich) in D_2O containing 0.9% NaCl. Diluted porphyrin solutions in PBS were obtained by adding 80 μL of porphyrin stock solution in D_2O or DMSO-*d6*

dx.doi.org/10.1021/jp403331n | J. Phys. Chem. B XXXX, XXX, XXX–XXX

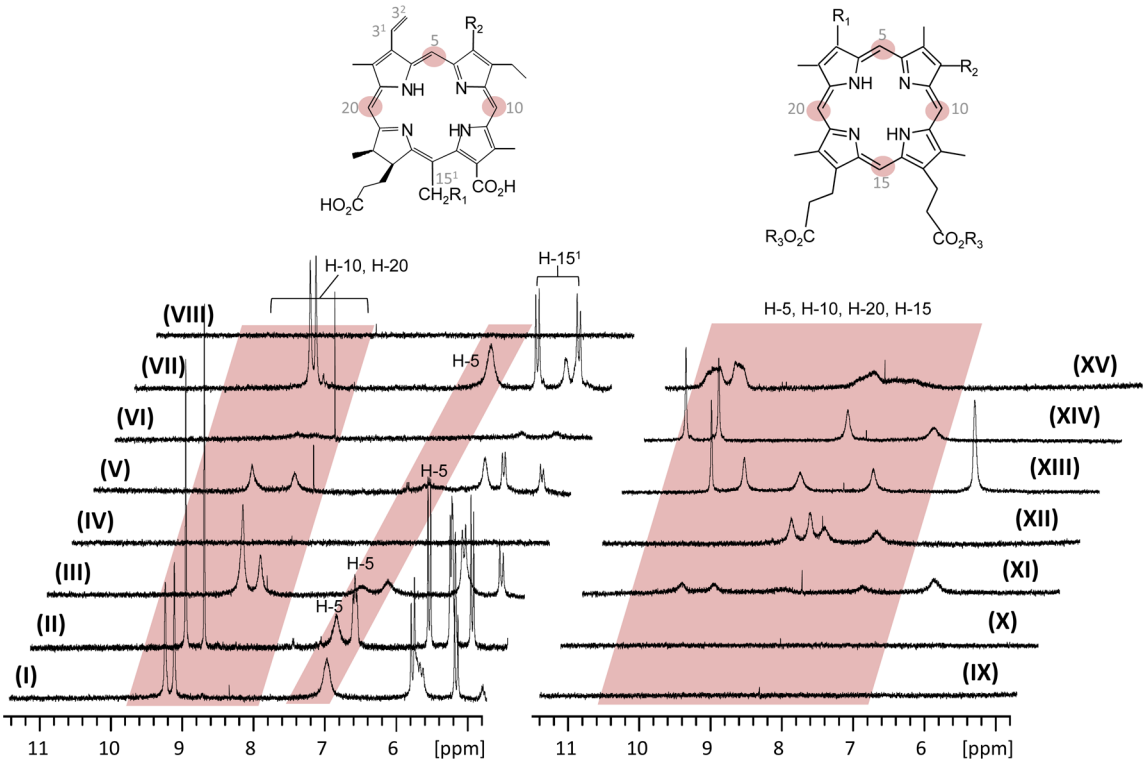

Figure 2. ^{1}H NMR spectra of porphyrinic compounds I–XV in PBS (1.76 mM, D_2O, pH 7). Spectral regions of the meso-proton resonances (H-5, H-10, H-15, H-20) are highlighted.

to 600 μL of PBS, yielding a porphyrin concentration of 1.76 mM.

Vesicle Preparation and Addition of Porphyrins. Unilamellar DOPC vesicle (50–60 nm in diameter) solutions (10 mM DOPC) in PBS at neutral pH were prepared by the extrusion method as previously described.[25] 500–600 μL of 10 mM DOPC solution in PBS was transferred to 5 mm NMR tubes (Wilmad), and aliquots of porphyrin stock solutions were added and mixed in the NMR tube to yield a molar ratio of porphyrin/DOPC of 0.025.

Preparation of DHPC Micelle Solutions and Addition of Porphyrins. DHPC micelle solutions in PBS (pH 7) were prepared at a DHPC concentration of 40 mM which is well above the critical micelle concentration (cmc) of 14–15 mM.[26] 500 μL of 40 mM DHPC solution in PBS was transferred to 5 mm NMR tubes, and 50 μL of porphyrin stock solutions was added and mixed in the NMR tube to yield a molar ratio of porphyrin/DHPC of 0.037.

Nuclear Magnetic Resonance (NMR) Spectroscopy. The NMR experiments were performed on two Bruker Avance II spectrometers operating at resonance frequencies of 500.13 and 400.13 MHz for ^{1}H nuclei, respectively. Both instruments are equipped with a 5 mm dual probe (BBI) for inverse detection with *z*-gradient coils. If not mentioned differently, all experiments were carried out at room temperature (298 K). Postprocessing of the NMR spectra was performed using the Bruker software Topspin 2.1. Fitting procedures were carried out using Origin, version 5.0 (Microcal Software, Inc.).

1D ^{1}H NMR Spectroscopy. The ^{1}H NMR spectra were recorded using a 1D NOESY presaturation sequence with spoil gradients for residual water suppression ("*noesygppr1d*" from the Bruker pulse-program library). Detailed acquisition and processing parameters for the NMR spectra are given in the Supporting Information. To follow the aggregate growth, the diluted porphyrin solutions in PBS were left standing at room temperature in the NMR tubes and ^{1}H NMR spectra were repeatedly recorded directly after sample preparation (day 0), and after 2, 6, and 9 days. For ^{1}H NMR measurements of DOPC vesicle solutions in the presence of porphyrins, a coaxial inner tube (WGS-5BL Wildmad) containing 60 μL of 1 mM TMSP in D_2O was inserted into each NMR sample tube as an internal reference. For ^{1}H NMR measurements of DHPC micelle solutions in the presence of porphyrins, the same parameters were used as for the diluted porphyrin solutions in PBS.

NMR Diffusion Measurements. Diffusion measurements were carried out on porphyrin stock solutions (15 mM) in D_2O (pH 9 by adding NaOD) or DMSO-*d6*. To determine the diffusion coefficients, 2D ^{1}H diffusion-ordered spectroscopy (DOSY) experiments were performed using a stimulated echo bipolar gradient pulse sequence with longitudinal eddy current delay and 2 spoil gradients ("*ledbpcpgp2sc*" from the Bruker pulse-program library).[27] To ensure a stable temperature, all diffusion measurements were carried out slightly above room temperature at T = 303 K. Normalized diffusion coefficients were determined as described in the Supporting Information.

Temperature Dependence of ^{1}H NMR Spectra. For probing the temperature dependence, ^{1}H NMR spectra of diluted porphyrin solutions in PBS were acquired using the 1D NOESY presaturation sequence. The field-frequency was locked on the deuterium resonance of deuterium oxide from PBS. The temperature was increased from room temperature (298 K) to 303 K and then stepwise (10 K increments) up to 343 K. The temperature dependence relative to DMSO-*d6* $\Delta(a(Hx))$ was determined for each of the assigned and resolved proton resonance shifts as described in the Supporting

dx.doi.org/10.1021/jp403331n | J. Phys. Chem. B XXXX, XXX, XXX–XXX

Information and plotted as bars for the individual porphyrinic compounds.

RESULTS AND DISCUSSION

For a comparative study, 15 chlorin and porphyrin compounds were selected all bearing an amphiphilic structure with ionizable substituents located on one side of the porphyrin macrocycle except for DPIXDS (XV). In 14 compounds, the ionizable groups consisted of at least two carboxylate substituents (I–XIII, XV), while compounds XIV and XV in addition bear two sulfate groups. Among the chlorin compounds (I–VIII), the main structural difference consisted in the nature of the substituent R_1 on the polar side of the amphiphilic molecule. Among the porphyrin compounds (IX–XV) on the other hand, the main structural difference consisted in the nature of the substituents R_1 and R_2 on the less polar side of the porphyrin macrocycle (Figure 1).

1. Aggregation of Porphyrins in Aqueous Buffer Solution. To study and compare the impact of the different substitution patterns on the aggregation behavior of the porphyrinic compounds under physiological conditions, the ^{1}H NMR spectra were analyzed in phosphate buffered saline (PBS, pH 7) solutions at the same concentrations (1.76 mM). In Figure 2, the aromatic regions of the corresponding ^{1}H NMR spectra are shown for compounds I–XV.

Typically, the aromatic meso-protons of unsymmetrical substituted natural chlorins and porphyrins give rise to 3 and 4 singlet resonances, respectively. Both upfield shift and signal broadening of the porphyrin NMR signals are indicative of the extent of aggregation in aqueous solution.[20] For compounds IV, VIII, IX, and X, no observable NMR resonances could be obtained under the selected conditions, suggesting the presence of highly aggregated species in solution,[28] in which no apparent precipitation could be observed. As expected, the corresponding chlorin and porphyrin derivatives were the least polar ones with IV and VIII bearing only two carboxylate groups and IX and X lacking additional polar substituents as compared to the remaining structures (Figure 1). Compounds V, VI, XI, XII, and XV gave rise to visible but strongly broadened NMR signals, indicating aggregates of intermediate size. For the remaining compounds (I–III, VII, XIII, and XIV), relatively sharp signals were observed. While line-broadening related to aggregate size appears more or less uniform, for these compounds, the meso-proton resonances were unequally broadened. This suggests the presence of self-assemblies such as dimers or oligomers involved in a dynamic process. Stronger line broadening and upfield shift were most pronounced for the H-5 resonance in the chlorin derivatives as previously described for I–III[25,29,30] and for the H-15 and H-20 resonances in the porphyrin derivatives. These upfield shifts are attributed to the ring current induced effects of neighboring porphyrin macrocycles in close proximity.[15] Furthermore, an exchange of intermediate rate on the NMR time scale between different forms like monomer/dimer or dimer/oligomer equilibria may contribute to the observed line broadening.[21,31] Aggregation of porphyrins bearing acidic or basic substituents is known to depend on their pK_a values and the pH of the surrounding medium. For compounds I–III, we have previously reported pK_a values between 4 and 8.3 for the individual carboxylate groups.[30] Other pK_a values for dicarboxylic porphyrins like HP and DP have been reported between 4 and 7.[32,33] Therefore, the carboxylate groups are partially deprotonated, while additional protonation of the inner pyrrole rings with pK_a values of 5 and lower[31,32,34] can be excluded in the physiologically relevant neutral pH range. Deprotonation of carboxylate groups seems to favor dimerization, while their protonation promotes the formation of larger supramolecular structures upon hydrogen bonding.[33] This became also evident from the diffusion constants, which were analyzed for the porphyrins in basic solutions (pH 9). The corresponding *D*-values as determined from diffusion ordered NMR spectroscopy (DOSY) are displayed in Figure 3 for those porphyrins

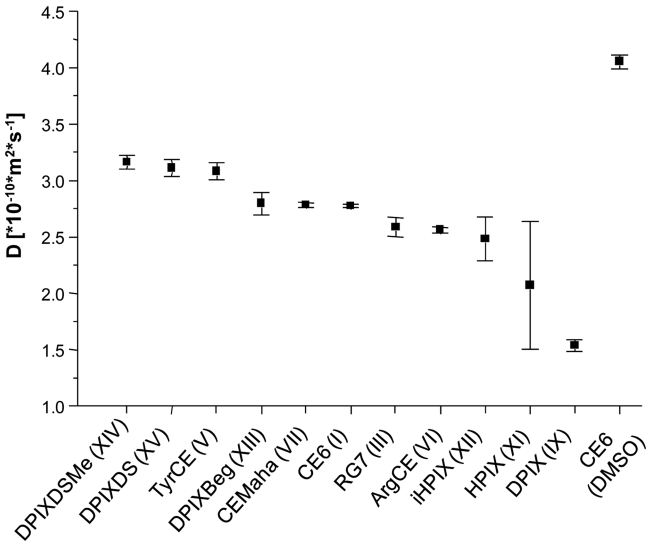

Figure 3. Diffusion coefficients of selected porphyrinic compounds in D_2O (15 mM, pH 9, 303 K); *D* values have been normalized to the molecular weight of CE6; for comparison: CE6 in DMSO, corrected for different viscosity.

giving rise to sufficiently intense signals. Since the diffusion coefficient correlates with the molecular weight, all *D*-values were normalized to the molecular weight of CE6 (I) in order to draw conclusions on the contribution of the aggregation number and aggregate size. Compared to the monomeric form of CE6 in DMSO with a *D*-value of 4.1×10^{-10} m^2/s, corrected for different viscosity, the *D*-values of the porphyrins in basic solution were all in the range between 1.5 and 3.2×10^{-10} m^2/s, indicating that mainly dimers or mixtures of dimers and monomers were formed. In neutral PBS, however, where the determination of exact *D*-values is hampered due to the broad and low-intensity signals, the formation of larger aggregates is likely resulting from partial protonation of the carboxylate side chains.

To probe the stability of the porphyrin self-assemblies formed in neutral PBS, selected compounds were left standing at room temperature over nine days. During this period, ^{1}H NMR spectra were acquired at three different time points, i.e., after 2, 6, and 9 days from each of the solutions. A more or less pronounced overall NMR signal intensity decrease was observed for all solutions, as shown for the aromatic protons in Figure 4. This suggests that the initially formed structures were not stable and that aggregate growth took place over time. In particular, the chlorin compounds exhibited a stronger signal intensity decrease than the porphyrin derivatives. Most likely, the porphyrin derivatives immediately formed higher aggregates in PBS solution as opposed to the chlorin derivatives so that their relative aggregate growth was smaller. In agreement with our observation, slow formation of large porphyrin assemblies

dx.doi.org/10.1021/jp403331n | J. Phys. Chem. B XXXX, XXX, XXX–XXX

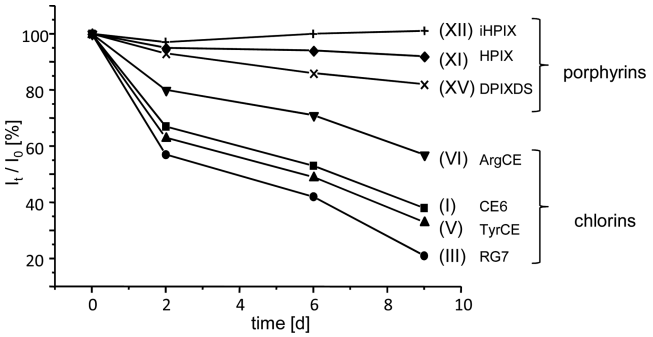

Figure 4. Aggregate growth of selected porphyrinic compounds in PBS (1.76 mM, D_2O, pH 7): Peak integrals (aromatic protons 8−12 ppm) at time t in % of the initial peak integral at time t = 0.

in aqueous solution has been previously reported.[20,33,35−38] For example, PPIX as an amphiphilic molecule has been postulated to form micelles at a certain concentration, while, at lower concentration depending on the pH, dimers are formed.[33,36] For synthetic porphyrins in aqueous solution, the nucleation step seemed to be an important factor preceding aggregate growth.[35,37] In particular, the presence of salts—as in PBS solution—enhances the hydrophobic interactions between porphyrin molecules[21] and thus promotes aggregation. In conclusion, all porphyrin and chlorin derivatives investigated in this study either spontaneously formed high aggregates or initially formed metastable di- or oligomers, tending to produce large self-assemblies over time in PBS solution.

2. Temperature Dependence of ^{1}H NMR Spectra of Porphyrins in Aqueous Solution. To study the structure of the chlorin and porphyrin aggregates in more detail, ^{1}H NMR spectra were recorded as a function of temperature for each of

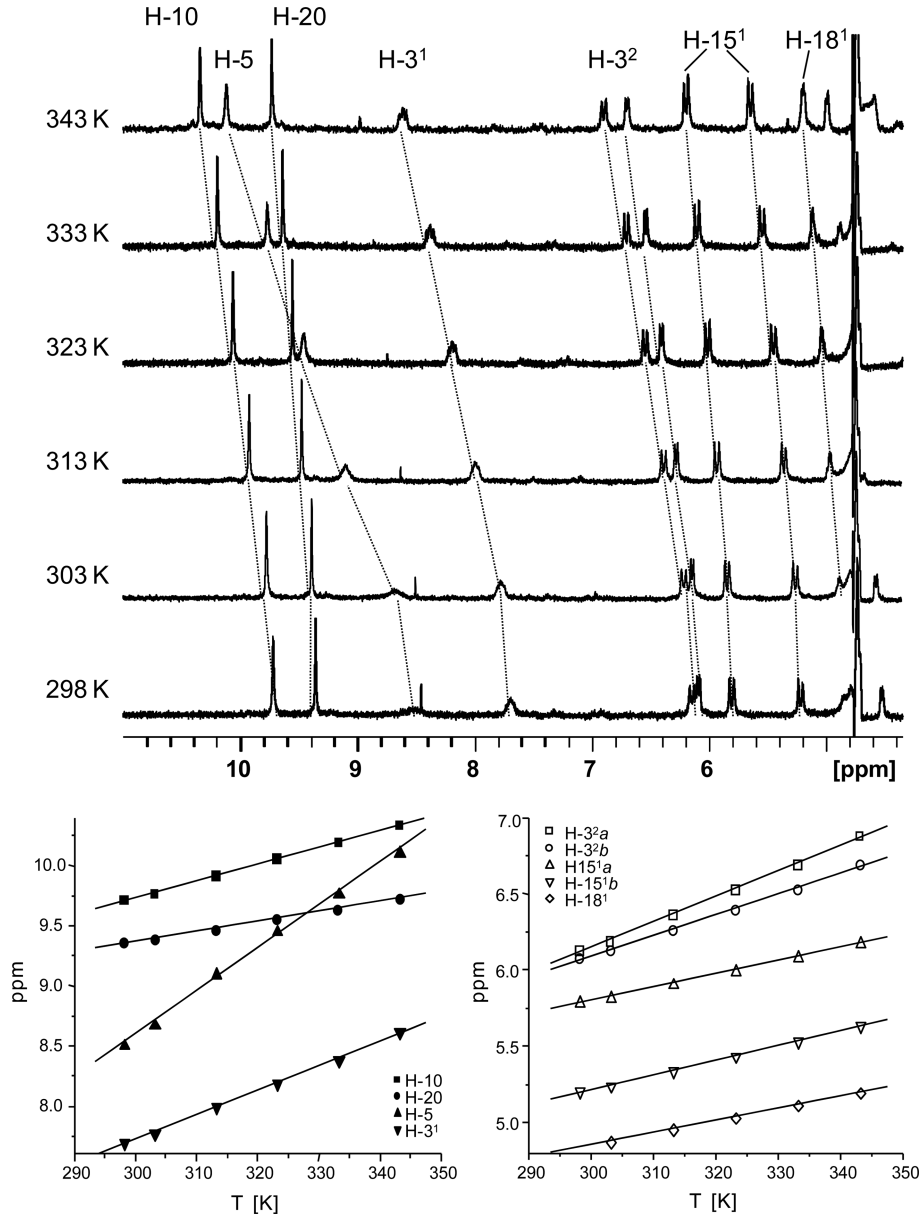

Figure 5. ^{1}H NMR spectra of the aromatic region of CE6 (I) in PBS (1.76 mM) at different temperatures. Chemical shift of aromatic resonances as a function of temperature; lines correspond to linear regression.

dx.doi.org/10.1021/jp403331n | J. Phys. Chem. B XXXX, XXX, XXX−XXX

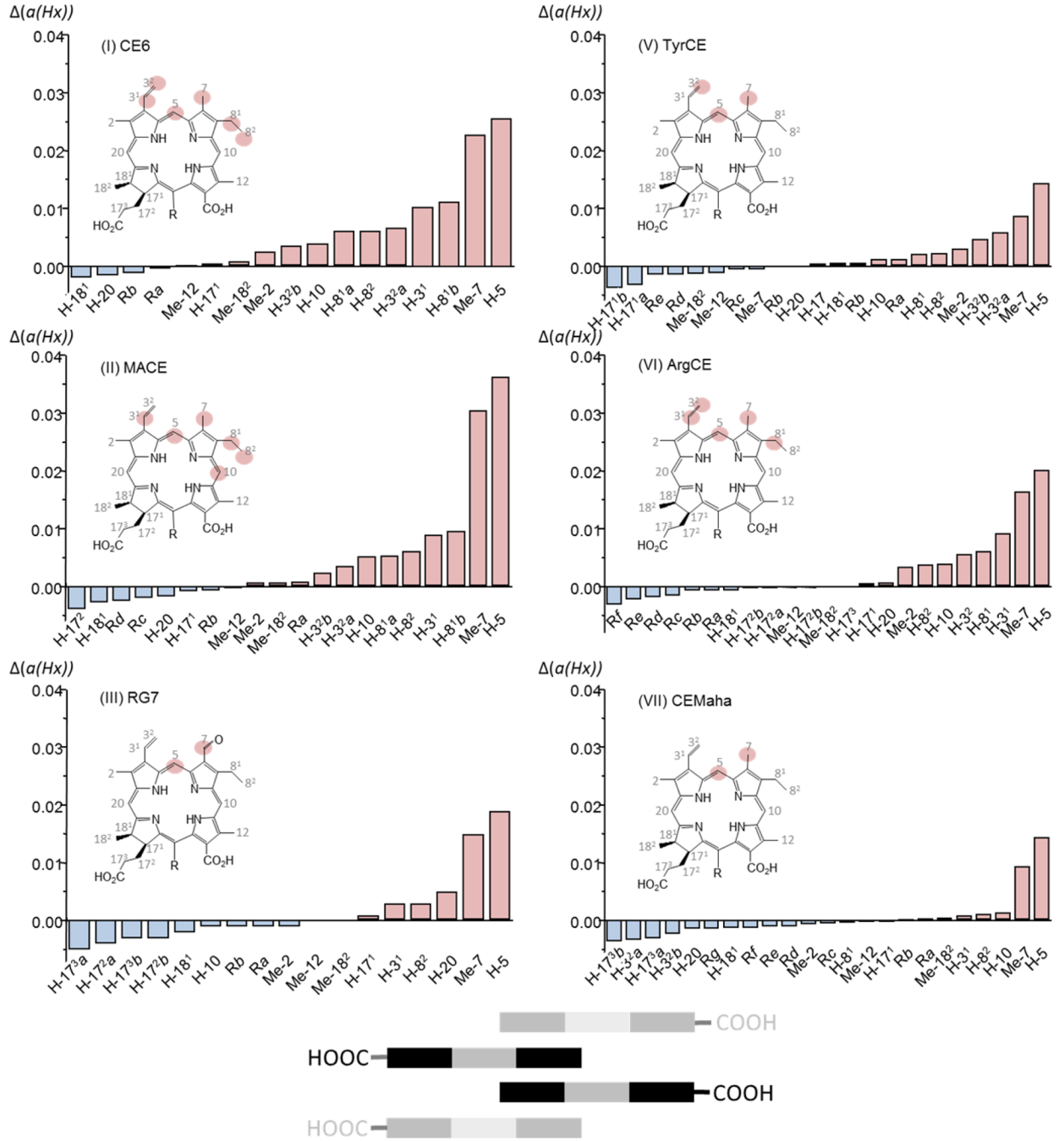

Figure 6. Temperature dependence of ^{1}H NMR resonance shifts expressed as the slope $\Delta(a(Hx))$ of linear regressions (δ versus T, corresponding to Figure 5) for the chlorin compounds I, II, III, V, VI, and VII and proposed scheme of the aggregate structure. Protons with $\Delta(a(Hx))$ values >0.005 are marked in the structures.

the compounds in PBS at a concentration of 1.76 mM. As an example, the aromatic regions of the temperature-dependent ^{1}H NMR spectra obtained for CE6 (I) are shown in Figure 5. Upon heating, a downfield shift was observed for all resonances, which was most pronounced for the signals of H-5 and H-3^1.

This became also evident when the chemical shift for each of the individual proton resonances was plotted as a function of temperature (Figure 5). Linear regressions gave a significantly steeper slope for the resonance of the H-5 meso-proton as compared to the remaining curves. In addition, the signals of H-5 and H-3^1, which appeared very broad at room temperature (298 K), exhibited a clear signal narrowing upon heating so that the multiplet structure of H-3^1 became visible at 343 K. The temperature-induced spectral changes can be interpreted as a result of disaggregation.[21] At increased temperature, the shifts move toward the position of the monomeric form which exists in DMSO. Both the extent and direction of chemical shift changes for the individual proton resonances provide information on the aggregate structure. Therefore, the chemical shifts of all resolved proton resonances for each of the investigated chlorin and porphyrin compounds were plotted versus temperature and the slopes were calculated from the corresponding linear regressions. In all cases, only downfield shifts were observed upon heating. The slopes $a(Hx)$ were

dx.doi.org/10.1021/jp403331n | J. Phys. Chem. B XXXX, XXX, XXX−XXX

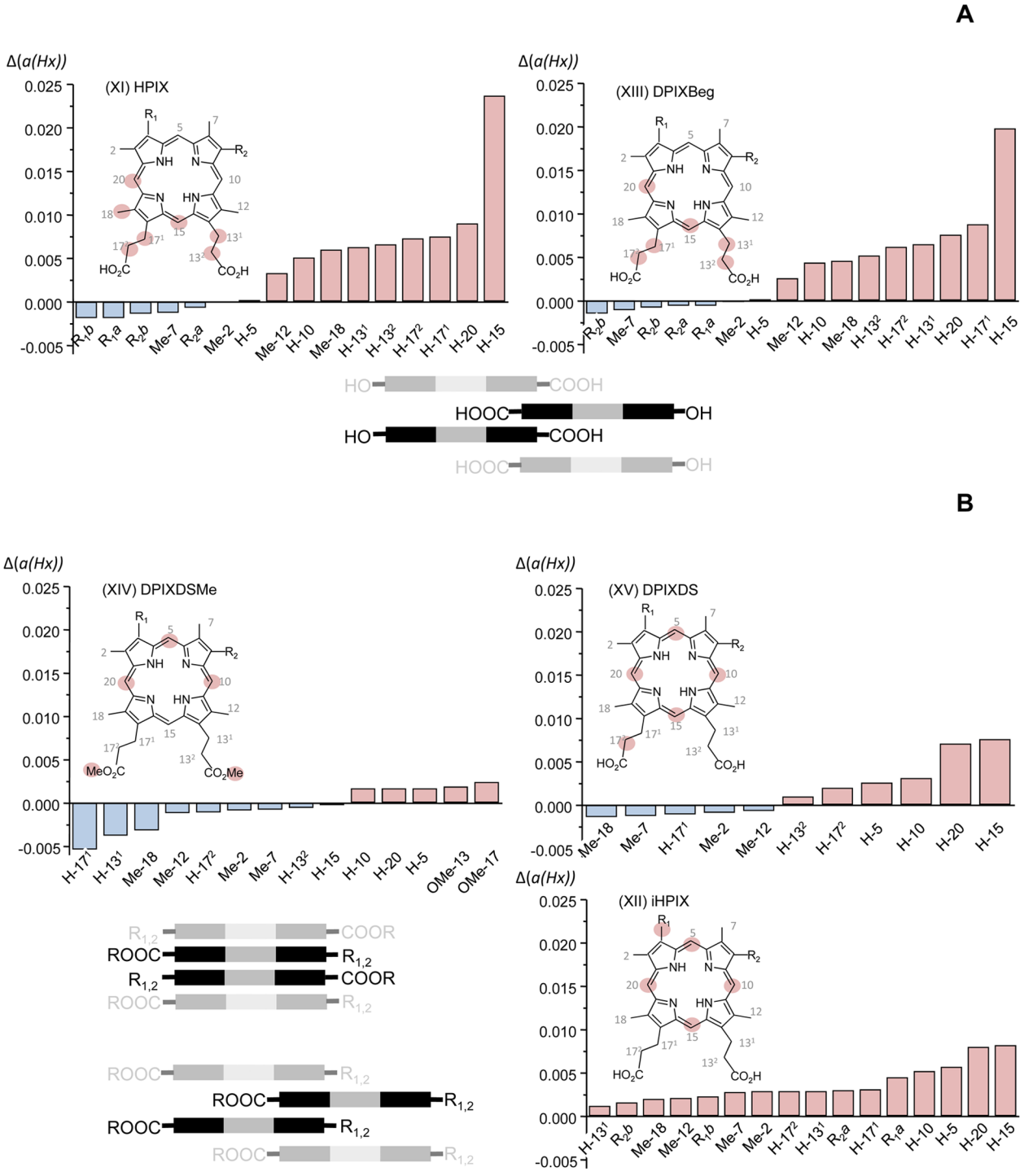

Figure 7. Temperature dependence of ^{1}H NMR resonance shifts expressed as the slope $\Delta(a(Hx))$ of linear regressions (δ versus T, corresponding to Figure 5) for the porphyrin compounds XI and XIII (A) and XII, XIV, and XV (B), and proposed schemes of the aggregate structures. Protons with $\Delta(a(Hx))$ values >0.005 (A) and with the five highest $\Delta(a(Hx))$ values (B) are marked in the structures, respectively.

compared to the one obtained for the temperature-dependent shift of the DMSO resonance in PBS, and the corresponding $\Delta(a(Hx))$ values were determined. On the basis of these $\Delta(a(Hx))$ values, aggregation maps for each investigated compound were then created as described in the Experimental Section and the Supporting Information. The resulting maps are shown in Figure 6 for the chlorin and in Figure 7 for the porphyrin compounds. The bar plots indicate which of the proton resonances exhibited the largest shifts relative to DMSO. NMR resonances with a stronger temperature dependent chemical shift are shown in red, while the others are shown in blue. The positions of protons with high aggregation shifts are indicated in the molecular structures. For the highly aggregated compounds IV, VIII, IX, and X not giving rise to observable NMR spectra at room temperature, no disaggregation could be observed upon heating.

3. Proposed Structure of Aggregates as Derived from the NMR Data. NMR aggregation shifts have proved to be a

dx.doi.org/10.1021/jp403331n | J. Phys. Chem. B XXXX, XXX, XXX−XXX

useful tool for the construction of aggregation maps of porphyrins and related compounds in the past.[22,39,40] Ring current induced upfield shifts observed for a given proton indicate its stacked proximity to a neighboring porphyrin ring. For all chlorin derivatives except for the highly aggregated IV and VIII, a very similar pattern was obtained (Figure 6), pointing to the same common aggregate structure. Each compound exhibited the largest shifts for the meso-proton H-5 and the methyl/methylene protons Me-7 at the hydrophobic side and only small changes for the protons at the hydrophilic side of the chlorin macrocycle. These asymmetrically induced shifts observed in all chlorin derivatives suggest an offset stacking geometry, as depicted in Figure 6. This geometry corresponds to the optimum dimer structure of amphiphilic porphyrins previously proposed.[33,41] In this structure, the pyrrole rings on the hydrophobic side of the macrocycle (rings A and B) overlap with the central cavity of the neighboring porphyrin ring, while the hydrophilic side chains extend toward the exterior aqueous phase. In chlorins, this orientation is in addition most likely supported by the partial hydration of ring D (7,8-dihydroporphine), reducing the ring current by about 10% as compared to porphyrins.[14] Such dimer structures are likely to propagate upon time by stacking of additional dimer building blocks, which is consistent with the observed aggregate growth for the chlorin compounds shown in Figure 4. These supra-molecular structures possibly can be stabilized by hydrogen bonds between the carboxylic acid side chains, which are partly protonated in the neutral pH range.

In contrast to the chlorin derivatives, for the porphyrin compounds XI and XIII, the largest shifts were observed for the resonance of the meso-proton H-15 on the opposite side of the porphyrin ring. Relatively strong aggregation shifts were also observed for the resonances of the H-20 and the propionate-CH_2 protons H-17^{1,2} and H-13^{1,2} (Figure 7). The strong asymmetry of induced shifts again suggests a partial overlap of neighboring porphyrin rings like in the chlorin compounds but this time only with their propionate bearing sides. The proposed aggregate structure shown in Figure 7 for porphyrins XI and XIII corresponds to a model previously suggested for PPIX-type porphyrins.[33] In this structure, the protonated carboxylate groups form hydrogen bonds with the central nitrogen atoms of the neighboring porphyrin ring. Thus, an overlap is confined only to the carboxylated side of the porphyrin ring, which is consistent with the observed chemical shift changes upon heating for XI and XIII. In contrast, a recent molecular dynamics simulation study proposed a dimer structure for deprotonated HPIX in water, showing an offset stacking with the hydroxyethyl groups partially overlapping.[42] The deviation from this model suggests either a considerable protonation of the carboxylate groups or a contribution of the experimental conditions like salt (PBS) or porphyrin concentration selected in the present study.

The remaining porphyrin derivatives XII, XIV, and XV formed a third class of aggregate structures. For these compounds, the observed aggregation shifts of all meso-proton resonances H-5, H-10, H-15, and H-20 were rather similar and not or hardly asymmetric. In addition, the overall magnitude of induced shifts was clearly smaller as compared to the previously discussed compounds. Different models are consistent with the observed aggregation shifts. One possibility is that stacks of parallel porphyrin rings resulting in H-type aggregate structures are formed. In this case, main contributions would derive from $\pi-\pi$-interactions, while the peripheral negatively charged sulfonate groups in compounds XIV and XV most likely point into opposite directions to avoid electrostatic repulsive interactions. Another possibility is the formation of slipped stacks of porphyrin rings with their substituents alternately pointing toward the core and the periphery, respectively. In this case, hydrogen bonds between peripheral substituents (−COOH or −OH) and the inner nitrogens might be involved. The proposed structure schemes are depicted in Figure 7.

In summary, the observed aggregation shifts propose a distinct difference in aggregate structure for the chlorins I−VIII on one side and the porphyrins IX−XV on the other side. Possible reasons for this difference are the following: (i) The enhanced amphiphilicity of the chlorin compounds with their rings A and B exhibiting a more hydrophobic character and their rings C and D a more hydrophilic character as compared to the porphyrin derivatives. (ii) The nature of the side chains on rings A and B in the porphyrin compounds XI−XV allows formation of hydrogen bonds and slightly increases the bulkiness of this side of the porphyrin macrocycle as compared with the chlorin compounds. (iii) The partial hydration of ring D in the chlorin compounds reduces their ring current and may thus rather promote stacking via overlapping of rings A and B (Figure 1).

4. Interaction of Porphyrin Aggregates with Phospholipid Bilayers and Monolayers. Since membranes belong to the main targets of porphyrinic photosensitizers,[4] it is of great interest how the aggregation behavior of a specific porphyrin affects its ability for membrane insertion. Both self-association and interaction with phospholipid (PL) bilayers form competitive processes for amphiphilic porphyrin compounds in aqueous solution. Which of these processes is emphasized depends on factors such as the membrane affinity of the compound of interest as well as the structure and stability of the existing aggregate in solution. Therefore, the interaction of all chlorin and porphyrin derivatives investigated in this study (I−XV) with phospholipid bilayers and monolayers was probed.

Small unilamellar vesicles (SUVs) composed of DOPC were used as membrane models. Previously, we have shown that the ^{1}H NMR spectroscopic resonances of the bilayer forming DOPC molecules can be used to monitor porphyrin−membrane interaction due to ring-current-induced spectral perturbations.[25,30,43] Initial association of the porphyrin with the outer membrane layer causes a split of the phospholipid *N*-methyl-choline resonance, as shown in Figure 8B with the upfield shifted part deriving from the outer monolayer. The magnitude of the split was found to depend on the amount of porphyrin in close proximity and thus provides information on its membrane surface affinity.[43] In Figure 8A, the induced split of the DOPC choline $-N^+(CH_3)_3$ resonance is given in ppm for each compound. Largest splits were caused by the chlorin compounds except for CE4 (VIII), indicating a higher membrane affinity for these compounds as compared to the porphyrin derivatives IX−XV. Electrostatic interactions between the negatively charged porphyrin carboxylate and the positively charged PL choline substituents are assumed to belong to the driving forces for initial porphyrin membrane interaction. Accordingly, corresponding pK_a values and the extent of amphiphilicity were found to modify these interactions.[30,43−45] The data presented in the current paper suggest that the aggregate structure is another important factor for porphyrin membrane interaction. The distinctly different

dx.doi.org/10.1021/jp403331n | J. Phys. Chem. B XXXX, XXX, XXX−XXX

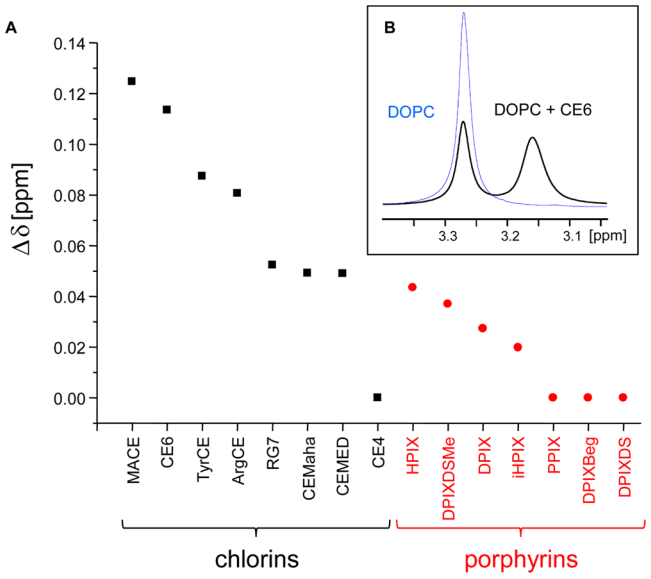

Figure 8. Initial chemical shift difference $\Delta\delta$ of the inner and outer DOPC choline $-N^+(CH_3)_3$ resonance of the DOPC bilayer after addition of porphyrinic compounds at a molar ratio of porphyrin/DOPC = 0.025 (10 mM DOPC in PBS, pH 7).

membrane affinity observed for chlorins and porphyrins cannot be explained on the basis of their monomeric structures. The aggregate structure proposed for the chlorin compounds (Figure 6) exhibits enhanced accessibility of the carboxylate substituents as compared to the aggregate structures proposed for the porphyrin compounds (Figure 7) where the carboxylate groups are located in overlapping regions of the aggregate. The relatively free accessibility of the carboxylate groups in the chlorin derivatives may thus promote their initial membrane surface association. Among the highly aggregated chlorins CEMED (IV) and CE4 (VIII), the aggregate structure of CEMED could at least partially be broken up in favor of membrane insertion, while for CE4 no membrane interaction could be detected (Figure 8). On the basis of the similarities of aggregation shifts found for all observable chlorin derivatives (Figure 6), it can be assumed that CEMED and CE4 aggregates exhibit the same building blocks, i.e., chlorin rings partially overlapping with their hydrophobic sides. For CE4, it may thus mainly be the aggregate size which hinders membrane interaction. Among the porphyrin derivatives (IX–XV) besides the highly aggregated PPIX, also DPIXBEG (XIII) and DPIXDS (XV) did not show any initial membrane surface affinity as derived from the lack of a split PL choline resonance (Figure 8A). In addition to the above-mentioned aggregate structure related reasons, this may also be due to the attenuated amphiphilicity of compounds XIII and XV as previously discussed.[43] Nevertheless, for the remaining porphyrin compounds, membrane interaction—less pronounced than for the chlorin derivatives—could be observed to some extent even for highly aggregated DPIX. In summary, membrane interaction seems to be modulated by interplay of various mutually dependent factors, among which the aggregate structure and size seem to have considerable contributions. In agreement with this, for highly diluted solutions of dicarboxylic porphyrins, a decrease in the entrance rate into DOPC bilayers has been attributed to porphyrin self-association.[32] Accordingly, the extent of self-aggregation of differently substituted tetraphenyl-porphyrin derivatives was recently found to be inversely correlated with their association kinetics to DMPC liposomes.[46]

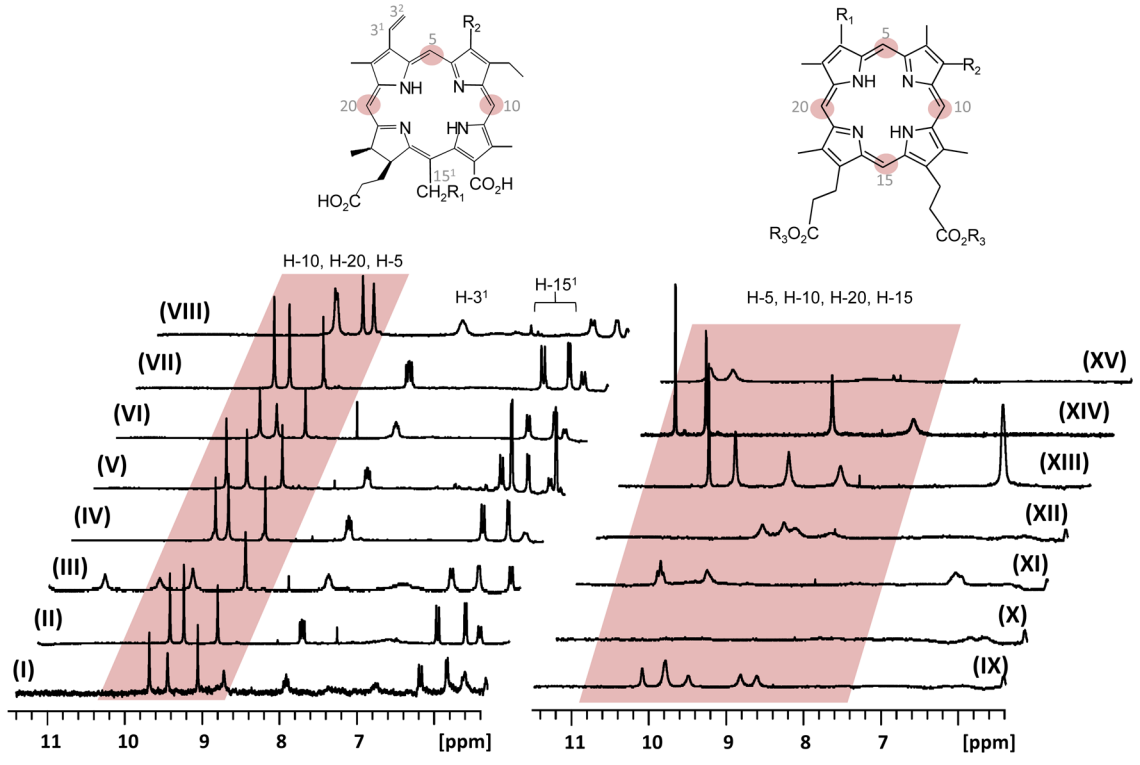

Figure 9. ^{1}H NMR spectra of porphyrinic compounds I–XV in DHPC micelles (40 mM in PBS, pH 7, molar ratio porphyrin/DHPC = 0.037). Spectral regions of the meso-proton resonances are highlighted.

dx.doi.org/10.1021/jp403331n | J. Phys. Chem. B XXXX, XXX, XXX–XXX

To date, it is not known if porphyrinic compounds only insert as monomers or also as dimers or oligomers into PL bilayers. Even large porphyrin assemblies are supposed to be taken up by cells most likely via endocytosis which are subsequently broken up inside the cell.[47] Both insertion of monomers into DMPC[46,48] and POPC[42] vesicles as well as dimer or oligomer insertion[30,49,50] have been reported for several free-base porphyrins. In addition, secondary dimerization[42] or formation of porphyrin rafts inside the membrane were suggested.[30,49,50]

Owing to the restricted dynamic properties of PL vesicles, the corresponding ^{1}H NMR vesicle spectra in the presence of porphyrins do not provide direct information on the porphyrin associated with the membrane due to strong signal broadening of the porphyrin resonances. Therefore, porphyrin interactions were probed in addition with structurally similar phospholipid micelles. The micelles were composed of dihexanoyl-*sn*-glycero-3-phosphocholine (DHPC), which due to their enhanced mobility allowed observation of porphyrin signals. In Figure 9, the ^{1}H NMR spectra obtained for all chlorin and porphyrin derivatives I–XV in the presence of DHPC micelles in PBS at porphyrin/DHPC molar ratios of 0.037 are shown.

In the aromatic region, there was no signal overlap of the porphyrin resonances with those of DHPC, which were only present in the 1–5 ppm spectral region. For the chlorin derivatives I–VIII, all meso-proton signals (H-5, H-10, H-20) appeared well resolved in the spectral region between 8.8 and 10 ppm as opposed to their spectral appearance solely in PBS (Figure 2). Both downfield shifts and signal narrowing indicated that all chlorin derivatives, even the highly aggregated species of CE4 (VIII), were monomerized by DHPC micelles. In contrast, for the porphyrin derivatives IX–XV, a monomerization could not be observed. No significant spectral changes occurred in the presence of DHPC micelles (Figure 9) as compared with the corresponding solutions in pure PBS (Figure 2). The shape and position of the four meso-proton resonances suggest that the porphyrin derivatives IX–XV still mainly exist as aggregates in the micellar solution. Nevertheless, slight downfield shifts or the emergence of NMR signals in the case of DPIX point toward weak interactions with the DHPC–micellar interface. The differences in micellar solution observed for the chlorin compounds on one hand and the porphyrin compounds on the other hand were in agreement with those obtained for the DOPC bilayer vesicles. Both systems, DHPC micelles and DOPC vesicles, exhibit the same headgroup regions but mainly differ in their hydrophobic chain lengths and dynamic properties. While the enhanced mobility of DHPC micelles allows breaking up even large aggregates, the initial affinity is governed by electrostatic interactions between PL headgroups and the porphyrinic side chains. Thus, the chlorin compounds seemed to comply best with the requirements for micellization regardless of their aggregate size. In contrast, the porphyrin derivatives exhibited a low affinity toward DHPC micelles despite the presence of carboxylate groups most likely because they are buried within the aggregate and not accessible for interacting with the DHPC headgroups. This finding supports the hypotheses drawn from the data obtained with PL bilayers; i.e., the aggregate structure and the resulting accessibility of carboxylate groups seem to contribute strongly to the membrane affinity.

CONCLUSION

In a systematic comparative study, a total of 15 carboxylated porphyrinic compounds comprising 8 derivatives of chlorin e6 and 7 derivatives of deuteroporphyrin IX were investigated with respect to their aggregation behavior and membrane affinity in PBS solution applying ^{1}H NMR spectroscopy. Aggregation maps could be derived, suggesting different aggregate structures for the chlorins on one side and the porphyrins on the other side. Even though additional complementary methods would be necessary to confirm a detailed aggregate structure, NMR has proved to be a powerful tool for unambiguously assigning submolecular regions either free or overlapping with neighboring molecules. The most important difference with respect to membrane interaction was the accessibility of the carboxylate groups which was enhanced for the chlorin derivatives.

The presented data demonstrate that the substitution pattern of the porphyrin macrocycle can have a strong impact on the aggregation behavior even for structurally similar compounds. Moreover, the results obtained with phospholipid bilayers and micelles suggest that the aggregate structure correlates with membrane interaction. In particular, the initial membrane surface association, which is governed by electrostatic interactions, is clearly enhanced if the aggregate structure allows free access to the carboxylate groups. This conclusion was strongly supported by the finding that only the chlorin derivatives were monomerized by DHPC micelles regardless of their aggregate size. Nevertheless, even though the chlorin compounds exhibited a higher membrane surface affinity, their membrane penetration may not be sufficient in each case. As previously reported, if strong electrostatic interactions between the PL headgroups and porphyrin substituents prevail, the porphyrin rather remains anchored at the membrane surface.[30,44,45]

The high tendency of porphyrins for self-association and the observed instability of dimers or oligomers in PBS solution demonstrate that the use of delivery particles may be indispensable in most cases. Accordingly, a focus in current research related to third generation photosensitizers is given to nanoparticles used as delivery vehicles for porphyrinic compounds.[5,12] With this respect, the knowledge of the aggregate structure, size, and stability for a specific porphyrin is important for the development or choice of efficient delivery vehicles. The current systematic study has thus formed a contribution to reveal the relationship between substitution pattern, self-association behavior, and membrane interaction.

ASSOCIATED CONTENT

Supporting Information

Additional experimental details are given. They include (A) NMR spectroscopy acquisition and processing parameters, (B) determination of $\Delta(a(Hx))$ values for the temperature-dependent chemical shifts, and (C) DOSY NMR parameters and the calculation of normalized diffusion coefficients. This material is available free of charge via the Internet at http://pubs.acs.org.

AUTHOR INFORMATION

Corresponding Author

*Phone: +41 031 631 3948. Fax: +41 031 631 3424. E-mail: martina.vermathen@ioc.unibe.ch.

Notes

The authors declare no competing financial interest.

dx.doi.org/10.1021/jp403331n | J. Phys. Chem. B XXXX, XXX, XXX–XXX

■ ACKNOWLEDGMENTS

We gratefully acknowledge the financial support obtained from the Swiss National Science Foundation (SNF), grant no. 200021-119691.

■ REFERENCES

(1) Ethirajan, M.; Chen, Y.; Joshi, P.; Pandey, R. K. The Role of Porphyrin Chemistry in Tumor Imaging and Photodynamic Therapy. *Chem. Soc. Rev.* **2011**, *40* (1), 340−362.

(2) Moreira, L. M.; dos Santos, F. V.; Lyon, J. P.; Maftoum-Costa, M.; Pacheco-Soares, C.; da Silva, N. S. Photodynamic Therapy: Porphyrins and Phthalocyanines as Photosensitizers. *Aust. J. Chem.* **2008**, *61* (10), 741−754.

(3) Mroz, P.; Yaroslavsky, A.; Kharkwal, G. B.; Hamblin, M. R. Cell Death Pathways in Photodynamic Therapy of Cancer. *Cancers* **2011**, *3* (2), 2516−2539.

(4) Bonneau, S.; Vever-Bizet, C. Tetrapyrrole Photosensitisers, Determinants of Subcellular Localisation and Mechanisms of Photodynamic Processes in Therapeutic Approaches. *Expert Opin. Ther. Pat.* **2008**, *18* (9), 1011−1025.

(5) Paszko, E.; Ehrhardt, C.; Senge, M. O.; Kelleher, D. P.; Reynolds, J. V. Nanodrug Applications in Photodynamic Therapy. *Photodiagn. Photodyn. Ther.* **2011**, *8* (1), 14−29.

(6) Chatterjee, D. K.; Fong, L. S.; Zhang, Y. Nanoparticles in Photodynamic Therapy: An Emerging Paradigm. *Adv. Drug Delivery Rev.* **2008**, *60* (15), 1627−1637.

(7) Delmarre, D.; Hioka, N.; Boch, R.; Sternberg, E.; Dolphin, D. Aggregation Studies of Benzoporphyrin Derivative. *Can. J. Chem.* **2001**, *79* (5−6), 1068−1074.

(8) Uchoa, A. F.; de Oliveira, K. T.; Baptista, M. S.; Bortoluzzi, A. J.; Iamamoto, Y.; Serra, O. A. Chlorin Photosensitizers Sterically Designed to Prevent Self-Aggregation. *J. Org. Chem.* **2011**, *76* (21), 8824−8832.

(9) Makhseed, S.; Ibrahim, F.; Bezzu, C. G.; McKeown, N. B. The Synthesis of Metal-Free Octaazaphthalocyanine Derivatives Containing Bulky Phenoxy Substituents to Prevent Self-Association. *Tetrahedron Lett.* **2007**, *48* (41), 7358−7361.

(10) Nyokong, T. Effects of Substituents on the Photochemical and Photophysical Properties of Main Group Metal Phthalocyanines. *Coord. Chem. Rev.* **2007**, *251* (13−14), 1707−1722.

(11) Maree, M. D.; Nyokong, T.; Suhling, K.; Phillps, D. Effects of Axial Ligands on the Photophysical Properties of Silicon Octaphenoxyphthalocyanine. *J. Porphyrins Phthalocyanines* **2002**, *6* (6), 373−376.

(12) Kepczynski, M.; Dzieciuch, M.; Nowakowska, M. Nanostructural Hybrid Sensitizers for Photodynamic Therapy. *Curr. Pharm. Des.* **2012**, *18* (18), 2607−2621.

(13) Abraham, R. J.; Eivazi, F.; Pearson, H.; Smith, K. M. Pi-Pi Aggregation in Metalloporphyrins - Causative Factors. *J. Chem. Soc., Chem. Commun.* **1976**, No. 17, 699−701.

(14) Abraham, R. J.; Smith, K. M.; Goff, D. A.; Lai, J. J. Nmr-Spectra of Porphyrins. 18. A Ring-Current Model for Chlorophyll Derivatives. *J. Am. Chem. Soc.* **1982**, *104* (16), 4332−4337.

(15) Abraham, R. J.; Smith, K. M. NMR-Spectra of Porphyrins. 21. Applications of the Ring-Current Model to Porphyrin and Chlorophyll Aggregation. *J. Am. Chem. Soc.* **1983**, *105* (18), 5734−5741.

(16) Hunter, C. A.; Sanders, J. K. M. The Nature of Pi-Pi Interactions. *J. Am. Chem. Soc.* **1990**, *112* (14), 5525−5534.

(17) Medforth, C. J. NMR Spectroscopy of Diamagnetic Porphyrins. In *The Porphyrin Handbook*; Kadish, K. M., Smith, K. M., Guilard, R., Eds.; Academic Press: San Diego, San Francisco, New York, Boston, London, Sydney, Tokyo, 2000; pp 1−80.

(18) Koehorst, R. B. M.; Hofstra, U.; Schaafsma, T. J. Solution Structure of Porphyrin Aggregates Determined by H-1-NMR Ring Current Shifts. 2. Conformations of Dimers and higher Aggregates of Water-Soluble Porphyrins. *Magn. Reson. Chem.* **1988**, *26* (2), 167−172.

(19) Hofstra, U.; Koehorst, R. B. M.; Schaafsma, T. J. Solution Structure of Porphyrin Aggregates Determined by H-1-Nmr Ring Current Shifts. 1. Heterodimers of Oppositely Charged Porphyrins. *Magn. Reson. Chem.* **1987**, *25* (12), 1069−1073.

(20) Rubires, R.; Crusats, J.; El Hachemi, Z.; Jaramillo, T.; Lopez, M.; Valls, E.; Farrera, J. A.; Ribo, J. M. Self-Assembly in Water of the Sodium Salts of Meso-Sulfonatophenyl Substituted Porphyrins. *New J. Chem.* **1999**, *23* (2), 189−198.

(21) Kano, K.; Fukuda, K.; Wakami, H.; Nishiyabu, R.; Pasternack, R. F. Factors Influencing Self-Aggregation Tendencies of Cationic Porphyrins in Aqueous Solution. *J. Am. Chem. Soc.* **2000**, *122* (31), 7494−7502.

(22) Chambrier, I.; Cook, M. J.; Mayes, D. A.; MacDonald, C. NMR Spectroscopic Evidence for the Self-Association of Some Asymmetrically Substituted Phthalocyanines in Solution. *J. Porphyrins Phthalocyanines* **2003**, *7* (6), 426−438.

(23) Serra, V. V.; Andrade, S. M.; Neves, M. G.; Cavaleiro, J. A.; Costa, S. M. J-Aggregate Formation in Bis-(4-carboxyphenyl)-porphyrins in Water: pH and Counterion Dependence. *New J. Chem.* **2010**, *34* (12), 2757−2765.

(24) Hosomizu, K.; Oodoi, M.; Umeyama, T.; Matano, Y.; Yoshida, K.; Isoda, S.; Isosomppi, M.; Tkachenko, N. V.; Lemmetyinen, H.; Imahori, H. Substituent Effects of Porphyrins on Structures and Photophysical Properties of Amphiphilic Porphyrin Aggregates. *J. Phys. Chem. B* **2008**, *112* (51), 16517−16524.

(25) Vermathen, M.; Vermathen, P.; Simonis, U.; Bigler, P. Time-Dependent Interactions of the Two Porphyrinic Compounds Chlorin e6 and Mono-L-aspartyl-chlorin e6 with Phospholipid Vesicles Probed by NMR Spectroscopy. *Langmuir* **2008**, *24* (21), 12521−12533.

(26) Lipfert, J.; Columbus, L.; Chu, V. B.; Lesley, S. A.; Doniach, S. Size and Shape of Detergent Micelles Determined by Small-Angle X-ray Scattering. *J. Phys. Chem. B* **2007**, *111* (43), 12427−12438.

(27) Wu, D.; Chen, A.; Johnson, C. S., Jr. An Improved Diffusion-Ordered Spectroscopy Experiment Incorporating Bipolar-Gradient Pulses. *J. Magn. Reson., Ser. A* **1995**, *115* (2), 260−264.

(28) Wu, J. J.; Li, N.; Li, K. A.; Liu, F. J-Aggregates of Diprotonated Tetrakis(4-sulfonatophenyl)porphyrin Induced by Ionic Liquid 1-Butyl-3-methylimidazolium Tetrafluoroborate. *J. Phys. Chem. B* **2008**, *112* (27), 8134−8138.

(29) Gomi, S.; Nishizuka, T.; Ushiroda, O.; Uchida, N.; Takahashi, H.; Sumi, S. The Structures of Mono-L-aspartyl Chlorin e6 and Its Related Compounds. *Heterocycles* **1998**, *48* (11), 2231−2243.

(30) Vermathen, M.; Marzorati, M.; Vermathen, P.; Bigler, P. pH-Dependent Distribution of Chlorin e6 Derivatives across Phospholipid Bilayers Probed by NMR Spectroscopy. *Langmuir* **2010**, *26* (13), 11085−11094.

(31) Choi, M. Y.; Pollard, J. A.; Webb, M. A.; Mchale, J. L. Counterion-Dependent Excitonic Spectra of Tetra(p-carboxyphenyl)-porphyrin Aggregates in Acidic Aqueous Solution. *J. Am. Chem. Soc.* **2003**, *125* (3), 810−820.

(32) Bonneau, S.; Maman, N.; Brault, D. Dynamics of pH-Dependent Self-Association and Membrane Binding of a Dicarboxylic Porphyrin: a Study with Small Unilamellar Vesicles. *Biochim. Biophys. Acta, Biomembr.* **2004**, *1661* (1), 87−96.

(33) Scolaro, L. M.; Castriciano, M.; Romeo, A.; Patane, S.; Cefali, E.; Allegrini, M. Aggregation Behavior of Protoporphyrin IX in Aqueous Solutions: Clear Evidence of Vesicle Formation. *J. Phys. Chem. B* **2002**, *106* (10), 2453−2459.

(34) Datta, A.; Dube, A.; Jain, B.; Tiwari, A.; Gupta, P. K. The Effect of pH and Surfactant on the Aggregation Behavior of Chlorin p(6): A Fluorescence Spectroscopic Study. *Photochem. Photobiol.* **2002**, *75* (5), 488−494.

(35) Scolaro, L. M.; Castriciano, M.; Romeo, A.; Mazzaglia, A.; Mallamace, F.; Micali, N. Nucleation Effects in the Aggregation of Water-Soluble Porphyrin Aqueous Solutions. *Physica A (Amsterdam, Neth.)* **2002**, *304* (1−2), 158−169.

(36) Brown, S. B.; Shillcock, M.; Jones, P. Equilibrium and Kinetic Studies of Aggregation of Porphyrins in Aqueous-Solution. *Biochem. J.* **1976**, *153* (2), 279−285.

(37) Schwab, A. D.; Smith, D. E.; Rich, C. S.; Young, E. R.; Smith, W. F.; de Paula, J. C. Porphyrin Nanorods. *J. Phys. Chem. B* **2003**, *107* (41), 11339−11345.
(38) Matsuzawa, H.; Kobayashi, H.; Maeda, T. Spectra and Mean Association Number of Porphyrin J Aggregate. *Bull. Chem. Soc. Jpn.* **2012**, *85* (7), 774−785.
(39) Hynninen, P. H.; Lotjonen, S. Effects of Pi-Pi Interactions on the H-1-Nmr Spectra and Solution Structures of Pheophytin A and A′ Dimers. *Biochim. Biophys. Acta* **1993**, *1183* (2), 374−380.
(40) Fabiano, A. S.; Allouche, D.; Sanejouand, Y. H.; Paillous, N. Synthesis of a New Cationic Pyropheophorbide Derivative and Studies of Its Aggregation Process in Aqueous Solution. *Photochem. Photobiol.* **1997**, *66* (3), 336−345.
(41) Fuhrhop, J. H.; Demoulin, C.; Boettcher, C.; Koning, J.; Siggel, U. Chiral Micellar Porphyrin Fibers with 2-Aminoglycosamide Head Groups. *J. Am. Chem. Soc.* **1992**, *114* (11), 4159−4165.
(42) Stepniewski, M.; Kepczynski, M.; Jamroz, D.; Nowakowska, M.; Rissanen, S.; Vattulainen, I.; Rog, T. Interaction of Hematoporphyrin with Lipid Membranes. *J. Phys. Chem. B* **2012**, *116* (16), 4889−4897.
(43) Marzorati, M.; Bigler, P.; Vermathen, M. Interactions between Selected Photosensitizers and Model Membranes: an NMR Classification. *Biochim. Biophys. Acta, Biomembr.* **2011**, *1808* (6), 1661−1672.
(44) Bronshtein, I.; Smith, K. M.; Ehrenberg, B. The Effect of pH on the Topography of Porphyrins in Lipid Membranes. *Photochem. Photobiol.* **2005**, *81* (2), 446−451.
(45) Kepczynski, M.; Ehrenberg, B. Interaction of Dicarboxylic Metal Loporphyrins with Liposomes. The Effect of pH on Membrane Binding Revisited. *Photochem. Photobiol.* **2002**, *76* (5), 486−492.
(46) Ibrahim, H.; Kasselouri, A.; You, C.; Maillard, P.; Rosilio, V.; Pansu, R.; Prognon, P. Meso-Tetraphenyl Porphyrin Derivatives: The Effect of Structural Modifications on Binding to DMPC Liposomes and Albumin. *J. Photochem. Photobiol., A* **2011**, *217* (1), 10−21.
(47) Kelbauskas, L.; Dietel, W. Internalization of Aggregated Photosensitizers by Tumor Cells: Subcellular Time-Resolved Fluorescence Spectroscopy on Derivatives of Pyropheophorbide-a Ethers and Chlorin e6 under Femtosecond One- and Two-Photon Excitation. *Photochem. Photobiol.* **2002**, *76* (6), 686−694.
(48) Andrade, S. M.; Teixeira, R.; Costa, S. M.; Sobral, A. J. Self-Aggregation of Free Base Porphyrins in Aqueous Solution and in DMPC Vesicles. *Biophys. Chem.* **2008**, *133* (1−3), 1−10.
(49) Ricchelli, F.; Gobbo, S.; Moreno, G.; Salet, C.; Brancaleon, L.; Mazzini, A. Photophysical Properties of Porphyrin Planar Aggregates in Liposomes. *Eur. J. Biochem.* **1998**, *253* (3), 760−765.
(50) Borovkov, V. V.; Anikin, M.; Wasa, K.; Sakata, Y. Structurally Controlled Porphyrin-Aggregation Process in Phospholipid Membranes. *Photochem. Photobiol.* **1996**, *63* (4), 477−482.